Electric Fields in Simulated Martian Dust Devils

E. L. Barth, *Southwest Research Institute, Boulder, CO, USA (ebarth@boulder.swri.edu)*, **W. M. Farrell**, *Solar System Exploration Division, NASA/Goddard Space Flight Center, Greenbelt,* **S. C. R. Rafkin**, *Southwest Research Institute, Boulder, CO, USA.*

Introduction: Electric fields measured in the vicinity of terrestrial dust devils are the result of triboelectric charging of individual dust grains, most of which occurs in the saltation layer within the first few centimeters of the surface. Once charged, some of these grains are injected further into the air where they are transported upward by atmospheric currents. Differential transport and gravitational sedimentation sorts the dust devil aerosols by size so that the smaller and predominantly negatively charged particles populate the higher portion of the disturbance while the larger, positively charged particles fall to the ground or remain in the lower portion of the vortex.

Dust charging studies using Mars soil simulant (Krauss et al. 2003; Sternovsky et al. 2002) suggest that the triboelectric charging of dust observed within terrestrial dust disturbances is very possible on Mars. The vertical velocities within Martian dust devils can lift the charged dust particles, the smallest particles, hundreds of meters or more above the surface in a coherent column creating a charge separation that may be large enough to produce significant electric fields. On Mars, electric fields are limited by large increases in atmospheric conductivity when they reach sufficient magnitude to ionize CO_2 and by electric discharges thought to occur at ~20 to 25 kV/m (Kok and Renno 2009).

We have integrated the dust devil dynamics studies of Michaels and Rafkin 2004 with the particle charging of Farrell et al. 2006 to create a model which can explore the charge environment throughout the lifecycle of a dust devil. Specifically, we have modified the Mars Regional Atmospheric Modeling System (MRAMS) to include charge distribution as a function of dust particle size and composition, provided by the Macroscopic Triboelectric Simulation (MTS) code.

Modeling: MRAMS is used to investigate the complex physics of regional, mesoscale, and microscale atmospheric phenomena on Mars (*e.g.* Rafkin et al. 2001). It is a 3-D, nonhydrostatic model, which permits the simulation of atmospheric flows with large vertical accelerations, such as dust devils (Michaels 2006).

Our simulations described here have been initialized homogeneously using temperature and wind profiles from a Viking 1 landing site mesoscale simulation (Fenton and Michaels 2010) at approximately 10:00 LMST (local mean solar time). We run the model over a 15 km x 15 km x 7 km grid with 100 m grid-spacing in x and y and a vertical grid that stretches with height, starting from a layer thickness of 4 m near the surface to a layer thickness of 150 m at the top (150 x 150 x 64 grid points).

MRAMS includes a number of microphysics routines which simulate the transport and microphysical interactions of dust aerosols. Dust sources are provided via a surface dust lifting scheme, and the sink of dust is sedimentation to the surface. The dust lifting scheme includes multi-size dust transport capability (Michaels 2006). The dust surface source is parameterized based on the work of Armstrong and Leovy 2005.

MTS is a 3-D particle code which quantifies charging associated with swirling, mixing dust grains (Farrell et al. 2003; Farrell et al. 2006). Grains of pre-defined sizes and compositions are placed in a simulation box and allowed to move under the influence of winds and gravity. The model tracks the movement of individual grains in prevailing (cyclostrophic) winds and charge exchange upon grain-grain collision.

We impose a compositional mix to maximize the triboelectric surface potential difference ($\Delta\Phi$) between larger and smaller grains. Specifically, we apply the grain-grain contact electrification algorithm presented in Desch and Cuzzi 2000. As a rule, we use $\Delta\Phi = 1.6$ V to simulate a mixture of smaller metallic and larger basaltic type particles. We also consider cases where we treat $\Delta\Phi$ as a free parameter by examining the degree of electrification and grain charge-size distribution for a range of values approaching zero (uniform composition).

Information describing each MTS dust particle (*i.e.,* charge, radius, and mass) is used to instruct the MRAMS dust lifting scheme for each MRAMS model grid-cell. The amount of charge on the MTS dust grains reflects the point where the dust grain movement has become non-collisional and so there is no longer charge exchange through grain-grain collision.

The MTS dust grain information is binned into the appropriate microphysics mass/radius bins (Fig. 1, top panel). A lognormal function is then fit to the charge profile (Fig. 1, bottom panel). The first and second moments of the charge distribution are implemented as dynamical tracers within MRAMS so that as the dust moves within the MRAMS domain, the charge distribution can be reconstructed for any grid point. The distribution of charge in an MRAMS

grid box will change as the size distribution of particles evolves due to the effects of winds and gravity. MRAMS keeps track of the charge density as a passive tracer. This can then be used to calculate an electric field from the Poisson equation.

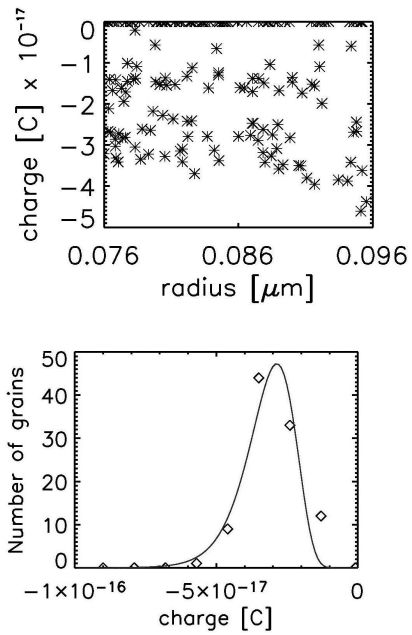

Figure 1. The top panel shows the raw output from MTS with the charge on each individual dust grain within in a given size range dictated by MRAMS. This information is used by MRAMS to bin the charge as shown in the bottomt panel. The charge distribution can be approximated by a log-normal distribution. MRAMS dynamic tracers are then (1) total particle number, (2) number of neutrals, (3) charge distribution first moment, and (4) charge distribution second moment.

Dust Devil Simulation Results: Electric fields are generated everywhere dust lifting occurs. The electric fields generated within the dust devils vary in strength due to three main factors: size of the dust particles, average charge density, and the number of dust particles in the atmosphere (controlled by the parameterized dust lifting efficiency). Because poorly constrained parameters can have a dramatic effect on the magnitude of the electric field, we have run several sensitivity tests. The parameter space that we have explored also includes some physically-implausible outliers in order to highlight their effect on the dust devil electric fields.

To isolate the effects of each of the variable parameters (size, charge, lifting), six cases were run and the results compared by looking at electric fields produced by the same dust devil in each model run. These cases are summarized in Table 1.

Table 1. Summary of dust devil sensitivity tests (in order of increasing electric field).

	Radius	Charge	Lifting eff.	Number* (cm^{-3})	Optical depth**	E-field* (V/m)
A	Small	Small	9e-8	11	5e-3	0.11
D	Small	Small	9e-7	110	5e-2	1.6
E	Small	Large	9e-8	16	5e-3	4.5
C	Large	large	9e-5	16	5e-1	39
F	large	small	9e-3	1100	5	200
B	large	large	9e-3	1600	50	3900

*Corresponding to maximum contour level in the plane 2 m above the surface

**Estimated visible-wavelength horizontal optical depth of the dust devil column

The dust particle size distributions were based on a known published distribution from Farrell et al. 2006 that possesses an adjustable power law particle size distribution. This power law type distribution was similar in nature to that used by Melnik and Parrot 1998. The dust particles are classified as either metals or basalts based on their charge sign (negative or positive, respectively). In the *small radius* case, the metals range from 0.05 – 0.2 μm in radius, with most particles having a radius of 0.1 μm; the basaltic particles are 0.2 – 10 μm in radius, with the peak of the size distribution at ~0.4 μm. Because the basalts are much less dense than the metals, the smaller basaltic particles fall at speeds comparable to the metal particles. Scaling both of the size distributions up by a factor of 10 (the *large radius* case) results in a greater vertical separation between the two populations of particles within a dust devil.

The charge on individual particles ranges from about 10^{-18} to 10^{-15} C. A number of neutral particles are also present. Figure 2 shows the average charge density distributions.

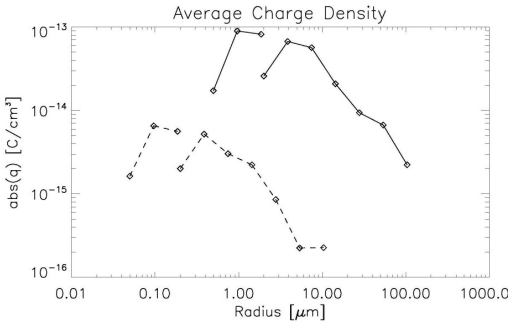

Figure 2. Average charge density distributions applied to the two size distribution cases described above. Absolute value is shown for the negatively charged particles.

The dust lifting efficiency regulates the amount of mass lifted and so controls the number of dust particles lifted into the atmosphere. The numerical value is specific to the dust lifting parameterization in the model (numerical values are listed in Table 1 to illustrate the difference between the cases; a more physical way to distinguish between the cases is to look at the number of particles in the dust devils).

Dust devils of reasonable optical depth in these simulations produce maximum electric fields of only 10-100 V/m. The dust devil case with a kV/m-class electric field is much more optically thick (τ ~ 50). For the smaller of the two particle size distributions used, the metallic particles are small enough that they do not contribute significantly to the visible optical depth. Because of this, we can increase the lifting efficiency of this case without increasing the optical depth or mass lifted as much as in the large particle case. We found that running the small particle case with a lifting efficiency of 10^{-5} will build up the electric field strength to 100 kV/m, which has been measured in some terrestrial dust devils. However, this requires more than 10,000 particles/cm^3 and results in having an optically thick dust devil (τ ~ 5).

Looking at the estimated visible-wavelength horizontal optical depth of the dust devil column, Case C might be a reasonable representation of Martian dust devils a few 100 m in diameter. Figure 3 shows a time series following the core of this dust devil over 150 seconds. The middle plots show E-fields clearly generated by the dust devil. The maximum electric fields are reached in the third panel (E-fields ~ 40 V/m).

Summary: We have enabled our Mars regional scale atmospheric model (MRAMS) to estimate an upper limit on electric fields generated by dust devil circulations by including charged particles as defined by the Macroscopic Triboelectric Simulation (MTS) code. Our MRAMS grid cell size makes our results most applicable to dust devils of a few hundred meters in diameter. We have run a number of simulations to understand the sensitivity of the electric field strength to the particle size and abundance and the amount of charge on each dust grain. Variations in these parameters scale the electric field produced by the dust devil.

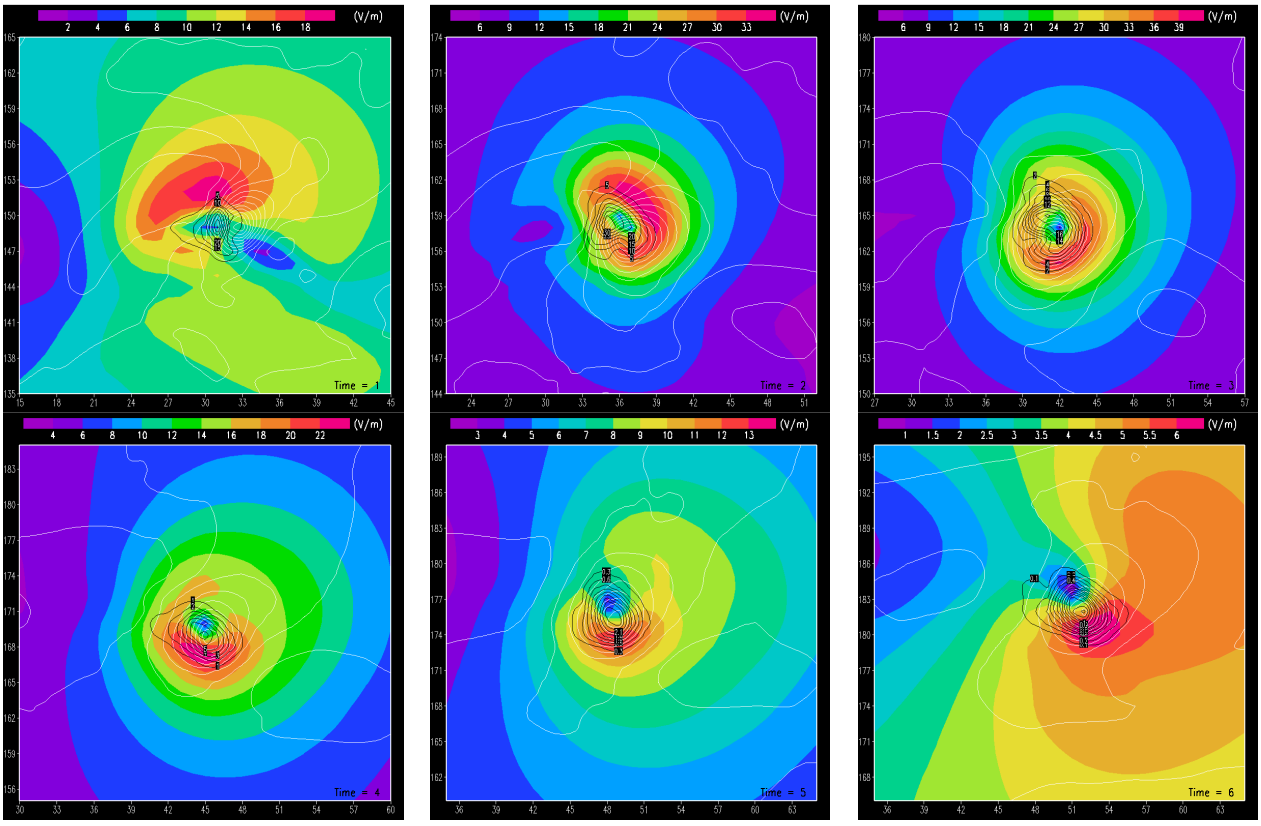

Figure 3. Time series plots of electric field magnitude (colored contours) in the vicinity of a dust devil (white pressure contours) at 30 second increments. Dust (#/cm^3) is also shown in the black contours. The time=1 and time=6 plots show interference from the E-fields generated in nearby gust fronts. The axes indicate coordinates in the xy-plane for a 1 km x 1 km area with the dust devil approximately centered. The dust devil is traveling in the +xy direction.

References:

Armstrong, J. C. and Leovy, C. B. (2005) "Long term wind erosion on Mars" Icarus 176, 57-74.

Desch, S. J. and Cuzzi, J. N. (2000) "The Generation of Lightning in the Solar Nebula" Icarus 143, 87-105.

Farrell, W. M. et al. (2003) "A simple electrodynamic model of a dust devil" Geophysical Research Letters 30, 2050.

Farrell, W. M. et al. (2006) "A model of the ULF magnetic and electric field generated from a dust devil" Journal of Geophysical Research 111, E11004

Fenton, L. K. and Michaels, T. I. (2010) "Characterizing the sensitivity of daytime turbulent activity on Mars with the MRAMS LES: Early results" International Journal of Mars Science and Exploration, vol. 4, p.159-171.

Krauss, C. E. et al. (2003) "Experimental evidence for electrostatic discharging of dust near the surface of Mars" New Journal of Physics, Volume 5, Issue 1, 70.

Kok, J. F. and Renno, N. O. (2009) "Electrification of windblown sand on Mars and its implications for atmospheric chemistry" Geophysical Research Letters 36, L05202.

Melnik, O. and Parrot, M. (1998) "Electrostatic discharge in Martian dust storms" Journal of Geophysical Research 103, 29107-29118.

Michaels, T. I. and S. C. R. Rafkin (2004) “Large eddy simulation of the convective boundary layer of Mars” Quarterly Journal of the Royal Meteorological Society 130, 1251-1274.

Michaels, T. I. (2006) "Numerical modeling of Mars dust devils: Albedo track generation" Geophysical Research Letters 33, L19S08.

Rafkin, S. C. R. et al. (2001) "The Mars Regional Atmospheric Modeling System: Model Description and Selected Simulations" Icarus 151, 228-256.

Sternovsky, Z. et al. (2002) "Contact charging of lunar and Martian dust simulants" Journal of Geophysical Research 107, 5105.